Arch. Met. Geoph. Biokl., Ser. B, 18, 287—294 (1970)

551.521.1:551.584:551.590.21

University of Virginia, Department of Environmental Sciences and Department of Astronomy, Charlottesville, Virginia, U. S. A.

Micrometeorological Observations of a Soil Surface during the Partial Phases of the Total Solar Eclipse of March 7, 1970

S. I. Outcalt and D. D. Meisel

With 2 Figures

Received June 8, 1970

Summary

Simultaneous observations of net radiation and temperature for the entire partial eclipse were obtained at a site with maximum obscuration of 92 % of the direct solar radiation. A strongly negative net radiation of —96 mly/min comparable to nocturnal conditions (—110 mly/min) was found at minimum light. Since low-light levels under normal daytime conditions (thick clouds) coincide with weak temperature gradients, organisms with both optical and thermal sensors may show a confused behavior under eclipse conditions. The contribution of direct solar radiation to the net radiation was computed using limb-darkened solar eclipse functions (included in an appendix) which show considerable departures from the uniform disk approximation.

Zusammenfassung

Mikrometeorologische Beobachtungen an einer Bodenoberfläche während der partiellen Phasen der totalen Sonnenfinsternis vom 7. März 1970

Gleichzeitige Beobachtungen der Strahlungsbilanz und der Temperatur wurden für die Dauer der partiellen Phase der Sonnenfinsternis an einem Beobachtungsort angestellt, an dem zur Zeit der maximalen Finsternis 92 % der direkten Sonnenstrahlung ausfielen. Eine stark negative Strahlungsbilanz von —96 mly/min, die nächtlichen Bedingungen (—110 mly/min) entspricht, wurde zum Zeitpunkt minimaler Einstrahlung vorgefunden. Da niedrige Lichtwerte unter normalen Tageslichtbedingungen (bei dichter Bewölkung) mit schwachen Temperaturgradienten zusammenfallen, können Organismen mit optischen und thermischen Sensoren unter den Bedingungen einer Sonnenfinsternis unregelmäßig reagieren. Der Beitrag der direkten Sonnenstrahlung zur Strahlungsbilanz wude mittels einer im Anhang angeführten Funktion berechnet, welche auf der Randverdunkelung der Sonne beruht. Diese Funktion zeigt bedeutsame Abweichungen gegenüber der Annahme einer gleichmäßigen Sonnenscheibe.

1. Introduction

Surface heating effects in the path of a solar eclipse have been briefly described by GRINGORTEN and KANTOR [1]. In this report, we describe detailed micrometeorological data acquired automatically at a previously established site where a considerable portion (92 %) but not all of the direct radiation was cut off during the March 7, 1970 total solar eclipse.

At the time of the event micrometeorological data were recorded on an 8-channel Brown Electronic Recorder as part of a programme of weather-soil frost observations at McCormick Observatory [2]. The site does not have a clear sunpath horizon and is located on a hilltop with an observatory dome 50 feet to the east and some trees and other structures to the south. As obstructions, these structures are not of great importance since the area of observation for the frost studies is a 1 meter square area of bare soil. The frost studies are thus concerned only with the environment of this test plot and no attempt is made to develop "representative data". During the partial eclipse the sun-path was relatively unobstructed, except by variable cloud cover at the beginning of the event, as no significant terrestrial obstructions were present in the near noon portion of the sunpath. A record of the detailed, near-surface effects of the partial eclipse was therefore acquired.

1. Astronomical Circumstances and the Incident Radiation

The direct solar contribution to the net radiation was computed by numerical integration using the limb-darkening coefficients listed by ALLEN [3], the eclipse parameters given by DUNCOMBE [4], and the solar irradiance parameters given by MOON [5] appropriately modified for earth-sun distance, water-vapor content, and revisions in the solar constant. Transmission in twelve wavelength ranges were considered: 0.30—0.33 μ, 0.33—0.36 μ, 0.36—0.39 μ, 0.39—0.42 μ, 0.42—0.47 μ, 0.47—0.55 μ, 0.70—0.90 μ, 0.90—1.25 μ, 1.25—1.75 μ, 1.75—2.5 μ, and 2.5 μ to 00. The standard conditions assumed were: pressure = 760 mm, precipitable water vapor = 0.75 cm, 300 dust particles/cm^3 and 0.28 atm-cm of ozone. These computations indicated that the direct solar contribution to the net radiation was 780 mly/min at the beginning of the eclipse (in the absence of clouds) and 580 mly/min at the end. At maximum obscuration (1334 EST) direct solar radiation still contributed 55 mly/min to the incident radiation.

The effect of ignoring solar limb-darkening in calculations of the direct solar radiation during a partial solar eclipse can be considerable, particularly for locations very near the path of totality. Since the results may be of interest for other investigations, we give the limb-darkened, as well as the uniform disk, eclipse functions for fifteen different wavelengths between 0.3 and 10 μ in the appendix. We have tabulated the ratio of the extra-atmospheric flux of the eclipsed sun to the extra-atmospheric flux of the unobscured sun as a function of wavelength and as a function of the apparent angular distance (in minutes of arc) between the center of the sun and the center of the moon. The angular distance between the sun-center and moon-center may be calculated as a function of time for any location within the zone of partial eclipse. Although these results apply strictly to the March 7, 1970 solar eclipse, use of these values properly scaled for other eclipses would be preferable to the uniform disk assumption. It can be seen from the appendix that limb-darkening "reddens" the direct solar radiation as the degree of obscuration increases. But even with atmospheric reddening, the radiation environment at maximum eclipse was *never* as shortwave deficient as would have been the case if atmospheric extinction *alone* had been responsible for the decreased level of direct radiation.

In the path of totality (2.4 km from the central line) light from the solar corona and the sky as observed at this eclipse by one of us (D. D. M.) was bright enough to read fine newsprint, even without prior dark adaptation. While skylight adds to visible light levels, calculation using the nocturnal surface temperature and the observed net radiation at 1930 EST show that (at maximum obscuration) skylight did not contribute more than nominally (less than 10 % of the total) to the radiation environment. After 1400 EST, however, intense reflections from the observatory dome increased the net radiation above the computed value of the direct solar beam.

3. Micrometeorological Observations

The eight channels were cycled every 4 minutes and printed on chart paper using a Brown Electronic Recorder. The following variables were recorded: (1) *Net Radiation* (a polythene shielded net radiometer calibrated for thermal radiation and excited by a bridge circuit; (2—5) *Wet and Dry Bulb temperatures* at 5 and 55 cm above a bare soil surface (aspirated radiation shielded fine thermocouples); (6) *Surface Temperature* (a thermocouple dusted with soil to provide a homogeneous surface albedo); (7) *Soil Temperature* (a thermocouple 1 cm below the soil surface); (8) *Heave Meter* (a bridge excited device for recording soil surface elevation changes by a resistance slide wire wiper circuit).

The recorded points on the chart paper were linked by straight lines and sampled at 5 minute intervals. This operation produced some smoothing of the data. It is recognized, that during the period variable cloud cover at the onset of the event, the sampling fre-

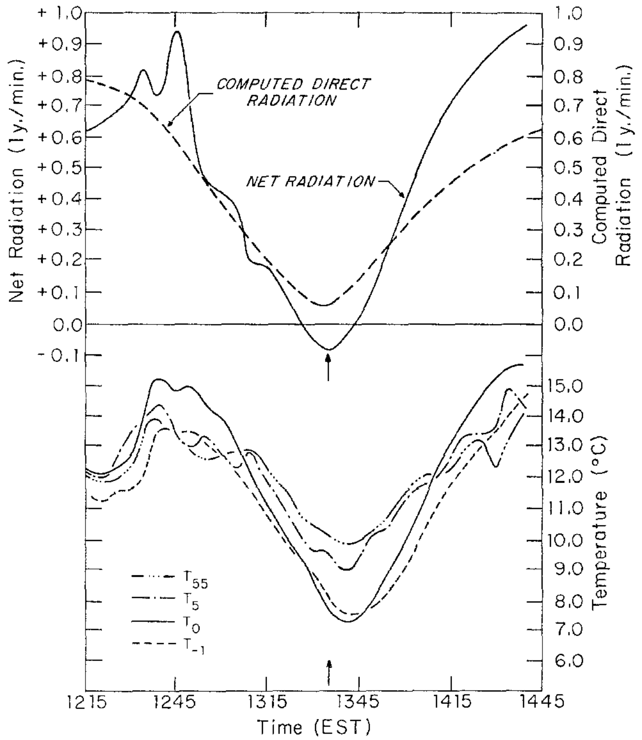

Fig. 1. Radiation and thermal data during the solar eclipse. Note the arrow which indicates maximum obscuration

quency was not dense enough to keep pace with rapid fluctuation which attended the alternate heating and cooling of the surface as the system was designed for more stable nocturnal conditions.

The record of radiation and temperature is presented as Fig. 1. The computed direct solar contribution to the net radiation is shown by the dashed line. To illustrate the magnitude and length of the thermal inversion in both the soil and air (which is characterized by heat flow toward the surface [+] from both above and below), the air and soil temperature differences between the near surface probes are plotted in Fig. 2. To eliminate the relatively high frequency effects of air turbulence in the record a smoothing function

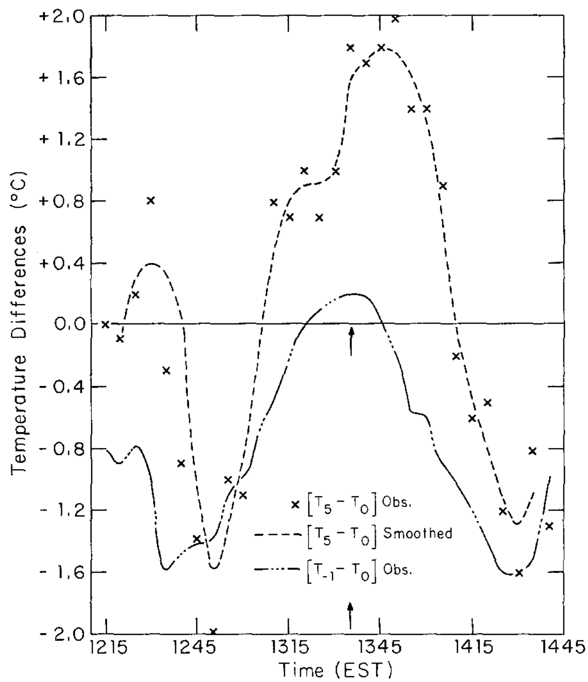

Fig. 2. Thermal gradients during the eclipse. Note that a positive gradient indicates an inversion with heat flowing toward the surface from the indicated level

(weighted .25, .50, .25) was applied to the air gradient data. The effect of solar reflections from the observatory dome can be seen after 1400 EST.

4. Conclusions

The net radiation, soil and air temperature inversions were similar to clear-sky nocturnal values, but at light levels (in the visible range) well in excess of those present under normal diurnal conditions. For example, the residual direct solar radiation at maximum eclipse for Charlottesville was comparable to the level on the central line of the eclipse some 4—5 minutes before the beginning of totality and after the end of totality. In spite of the fact that the sun was not completely covered, the net radiation balance with clear skies at maximum obscuration was strongly negative (—96 mly/min) nearly equivalent to the minimum (—110 mly/min) observed during nocturnal periods which bracketed the day of the eclipse.

Under normal daytime circumstances, low levels of visible light coincide with total stratus cloud cover and under such conditions the solar radiation (slightly positive) is nearly balanced by thermal radiation (slightly negative). The net result is a weak positive radiation budget accompanied by very weak temperature gradients above and below the soil surface Organisms capable of evaluating both optical and thermal information recognize such a correlation (low light, weak gradients) as a "normal" daylight condition. The same organisms presented with the unusual environment of a partial solar eclipse (low light, strong thermal gradients near the surface) may react in a very confused way. The work suggests that future investigations of biological reactions during solar eclipses should include coordinated studies of the thermal, as well as the optical, environment.

Acknowledgment

The work including the computations of the direct solar radiation was supported under National Science Foundation Institution Subgrant (70-290 L-A), to one of us (S. I. O.). We also wish to thank Mr. WILLIAM H. DANCY, Jr., and Mr. JASPER MOYERS of the Research Laboratories for Engineering Sciences for their aid in constructing and maintaining the micrometeorological equipment.

Appendix

The table lists the ratio of the extra-atmospheric residual eclipse flux $(F_\lambda)\ e$ to the extra-atmospheric solar flux outside eclipse $(F_\lambda)\ o$. For a uniform disk and limb-darkened disk for 15 wavelengths from $0.3\ \mu$ to $10\ \mu$ for eighty different apparent angular sun-center to moon-center distances from 0.5 of arc to 32.5 of arc. The limb-darkening coefficients for the sun listed by ALLEN [3] were used. In addition, we have listed the ratio of the total incident eclipse solar radiation (without sky light) to the uneclipsed value for a sun altitude of 45^0 after passing through an atmosphere with the properties listed in the text except that the precipitable water is 2 cm

RATIO OF Ḟλ (eclipsed) TO Fλ (uneclipsed)

d	Uniform Disk	0.32μ	0.35μ	0.37μ	0.40μ	0.45μ	0.50μ	0.60μ	0.80μ	1.00μ	1.5μ	2.0μ	3.0μ	5.0μ	10.0μ	$\frac{\Sigma(F\lambda)e}{\Sigma(F\lambda)o}$
0.5'	0.0012	0.0003	0.0003	0.0003	0.0003	0.0004	0.0005	0.0006	0.0007	0.0008	0.0009	0.0009	0.0010	0.0011	0.0011	0.0007
0.9'	0.0136	0.0042	0.0048	0.0052	0.0049	0.0057	0.0066	0.0078	0.0093	0.0099	0.0108	0.0112	0.0118	0.0125	0.0129	0.0087
1.3'	0.0284	0.0106	0.0118	0.0126	0.0120	0.0136	0.0153	0.0175	0.0203	0.0215	0.0231	0.0240	0.0250	0.0263	0.0270	0.0192
1.7'	0.0437	0.0184	0.0204	0.0215	0.0206	0.0230	0.0254	0.0286	0.0325	0.0342	0.0365	0.0376	0.0391	0.0408	0.0418	0.0308
2.1'	0.0593	0.0274	0.0300	0.0315	0.0303	0.0334	0.0365	0.0405	0.0453	0.0476	0.0504	0.0518	0.0536	0.0558	0.0569	0.0432
2.5'	0.0750	0.0374	0.0406	0.0424	0.0410	0.0447	0.0484	0.0530	0.0588	0.0614	0.0647	0.0663	0.0684	0.0708	0.0722	0.0484
2.9'	0.0908	0.0482	0.0520	0.0541	0.0523	0.0567	0.0609	0.0661	0.0726	0.0755	0.0793	0.0811	0.0834	0.0861	0.0876	0.0698
3.3'	0.1066	0.0597	0.0640	0.0664	0.0644	0.0693	0.0739	0.0797	0.0868	0.0900	0.0941	0.0961	0.0986	0.1015	0.1032	0.0837
3.7'	0.1224	0.0719	0.0766	0.0793	0.0770	0.0824	0.0875	0.0936	0.1012	0.1047	0.1092	0.1112	0.1139	0.1167	0.1187	0.0980
4.1'	0.1382	0.0846	0.0898	0.0927	0.0901	0.0960	0.1013	0.1079	0.1160	0.1196	0.1244	0.1265	0.1293	0.1324	0.1343	0.1125
4.5'	0.1540	0.0979	0.1034	0.1065	0.1038	0.1100	0.1157	0.1225	0.1309	0.1347	0.1400	0.1419	0.1448	0.1481	0.1500	0.1273
4.9'	0.1698	0.1116	0.1175	0.1208	0.1178	0.1244	0.1303	0.1373	0.1460	0.1500	0.1551	0.1573	0.1604	0.1637	0.1657	0.1423
5.3'	0.1856	0.1258	0.1320	0.1354	0.1323	0.1391	0.1452	0.1524	0.1613	0.1653	0.1707	0.1729	0.1760	0.1794	0.1814	0.1575
5.7'	0.2013	0.1404	0.1468	0.1503	0.1471	0.1541	0.1603	0.1677	0.1768	0.1808	0.1863	0.1886	0.1916	0.1950	0.1970	0.1728
6.1'	0.2170	0.1552	0.1619	0.1655	0.1622	0.1694	0.1757	0.1832	0.1923	0.1964	0.2019	0.2043	0.2073	0.2107	0.2127	0.1683
6.5'	0.2327	0.1705	0.1772	0.1810	0.1776	0.1849	0.1912	0.1988	0.2079	0.2121	0.2176	0.2200	0.2229	0.2264	0.2284	0.2039
6.9'	0.2483	0.1861	0.1930	0.1967	0.1933	0.2006	0.2070	0.2145	0.2237	0.2278	0.2334	0.2357	0.2387	0.2421	0.2440	0.2197
7.3'	0.2639	0.2019	0.2088	0.2127	0.2091	0.2165	0.2229	0.2304	0.2395	0.2436	0.2492	0.2514	0.2544	0.2578	0.2597	0.2355
7.7'	0.2795	0.2180	0.2250	0.2288	0.2252	0.2326	0.2389	0.2464	0.2554	0.2595	0.2650	0.2672	0.2701	0.2734	0.2753	0.2514
8.1'	0.2950	0.2343	0.2412	0.2450	0.2415	0.2489	0.2551	0.2625	0.2713	0.2753	0.2808	0.2830	0.2858	0.2890	0.2909	0.2674
8.5'	0.3104	0.2508	0.2577	0.2614	0.2579	0.2652	0.2713	0.2786	0.2873	0.2912	0.2966	0.2987	0.3015	0.3046	0.3064	0.2834
8.9'	0.3259	0.2675	0.2743	0.2780	0.2745	0.2817	0.2877	0.2948	0.3033	0.3071	0.3124	0.3144	0.3171	0.3202	0.3220	0.2995
9.3'	0.3412	0.2843	0.2910	0.2946	0.2912	0.2983	0.3041	0.3110	0.3193	0.3230	0.3281	0.3301	0.3328	0.3357	0.3374	0.3156
9.7'	0.3565	0.3013	0.3078	0.3114	0.3080	0.3149	0.3206	0.3273	0.3353	0.3389	0.3439	0.3458	0.3483	0.3512	0.3528	0.3318
10.1'	0.3718	0.3184	0.3247	0.3282	0.3249	0.3316	0.3371	0.3436	0.3513	0.3548	0.3596	0.3614	0.3639	0.3667	0.3682	0.3479
10.5'	0.3870	0.3356	0.3417	0.3451	0.3419	0.3483	0.3536	0.3599	0.3673	0.3707	0.3753	0.3771	0.3794	0.3821	0.3835	0.3640
10.9	0.4021	0.3528	0.3587	0.3619	0.3589	0.3651	0.3702	0.3762	0.3833	0.3865	0.3909	0.3926	0.3948	0.3974	0.3988	0.3801
11.3'	0.4171	0.3702	0.3758	0.3789	0.3760	0.3819	0.3867	0.3924	0.3992	0.4023	0.4065	0.4082	0.4102	0.4127	0.4140	0.3962
11.7'	0.4321	0.3875	0.3929	0.3958	0.3930	0.3987	0.4033	0.4087	0.4151	0.4180	0.4221	0.4236	0.4256	0.4279	0.4291	0.4122
12.1'	0.4470	0.4049	0.4100	0.4128	0.4101	0.4155	0.4198	0.4249	0.4310	0.4338	0.4376	0.4390	0.4409	0.4430	0.4442	0.4283
12.5'	0.4618	0.4223	0.4271	0.4297	0.4272	0.4323	0.4363	0.4411	0.4468	0.4494	0.4530	0.4543	0.4561	0.4581	0.4592	0.4443
12.9'	0.4765	0.4397	0.4442	0.4466	0.4443	0.4490	0.4528	0.4573	0.4626	0.4650	0.4683	0.4696	0.4712	0.4731	0.4741	0.4602
13.3'	0.4912	0.4571	0.4612	0.4635	0.4613	0.4657	0.4692	0.4733	0.4783	0.4805	0.4836	0.4847	0.4862	0.4880	0.4890	0.4761
13.7'	0.5058	0.4744	0.4782	0.4803	0.4783	0.4823	0.4855	0.4894	0.4939	0.4959	0.4988	0.4998	0.5012	0.5028	0.5037	0.4918
14.1'	0.5203	0.4917	0.4952	0.4970	0.4953	0.4989	0.5018	0.5053	0.5094	0.5113	0.5138	0.5148	0.5161	0.5176	0.5184	0.5076
14.5'	0.5346	0.5089	0.5120	0.5137	0.5121	0.5154	0.5180	0.5211	0.5249	0.5266	0.5289	0.5298	0.5309	0.5322	0.5330	0.5232
14.9'	0.5489	0.5260	0.5288	0.5303	0.5289	0.5318	0.5341	0.5369	0.5402	0.5417	0.5438	0.5446	0.5456	0.5468	0.5474	0.5387
15.3'	0.5631	0.5431	0.5455	0.5468	0.5455	0.5480	0.5501	0.5526	0.5555	0.5568	0.5586	0.5593	0.5602	0.5612	0.5618	0.5542
15.7'	0.5772	0.5600	0.5620	0.5631	0.5621	0.5642	0.5660	0.5681	0.5706	0.5717	0.5733	0.5739	0.5747	0.5756	0.5761	0.5695
16.1'	0.5912	0.5768	0.5784	0.5794	0.5785	0.5803	0.5818	0.5835	0.5856	0.5866	0.5879	0.5884	0.5890	0.5898	0.5902	0.5847
16.5'	0.6051	0.5934	0.5948	0.5955	0.5948	0.5962	0.5974	0.5988	0.6005	0.6013	0.6023	0.6028	0.6033	0.6039	0.6042	0.5998
16.9'	0.6668	0.6669	0.6669	0.6669	0.6669	0.6669	0.6669	0.6668	0.6668	0.6668	0.6668	0.6668	0.6668	0.6668	0.6668	0.6668
17.3'	0.6726	0.6731	0.6721	0.6730	0.6731	0.6730	0.6730	0.6728	0.6728	0.6727	0.6727	0.6727	0.6726	0.6726	0.6726	0.6728
17.7'	0.6790	0.6803	0.6802	0.6800	0.6802	0.6800	0.6798	0.6797	0.6795	0.6794	0.6793	0.6792	0.6792	0.6791	0.6791	0.6796
18.1'	0.6862	0.6885	0.6881	0.6880	0.6881	0.6878	0.6876	0.6872	0.6870	0.6869	0.6866	0.6865	0.6865	0.6864	0.6863	0.6871
18.5'	0.6939	0.6975	0.6970	0.6967	0.6970	0.6965	0.6961	0.6957	0.6952	0.6950	0.6946	0.6945	0.6943	0.6942	0.6941	0.6954
18.9'	0.7023	0.7073	0.7066	0.7062	0.7066	0.7059	0.7054	0.7048	0.7041	0.7038	0.7033	0.7032	0.7030	0.7027	0.7026	0.7044
19.3'	0.7113	0.7179	0.7170	0.7165	0.7170	0.7160	0.7153	0.7145	0.7136	0.7132	0.7126	0.7124	0.7121	0.7118	0.7117	0.7140
19.7'	0.7207	0.7291	0.7280	0.7274	0.7280	0.7268	0.7259	0.7249	0.7237	0.7232	0.7224	0.7222	0.7218	0.7214	0.7212	0.7242
20.1'	0.7307	0.7409	0.7395	0.7388	0.7395	0.7381	0.7370	0.7358	0.7343	0.7337	0.7328	0.7324	0.7320	0.7315	0.7313	0.7350
20.5'	0.7410	0.7532	0.7516	0.7507	0.7515	0.7499	0.7486	0.7471	0.7454	0.7446	0.7435	0.7432	0.7427	0.7421	0.7418	0.7462
20.9'	0.7518	0.7658	0.7639	0.7629	0.7639	0.7620	0.7605	0.7588	0.7569	0.7560	0.7547	0.7543	0.7537	0.7530	0.7527	0.7578
21.3'	0.7628	0.7787	0.7766	0.7754	0.7766	0.7744	0.7728	0.7708	0.7686	0.7676	0.7662	0.7656	0.7650	0.7642	0.7638	0.7696
21.7'	0.7741	0.7917	0.7894	0.7881	0.7893	0.7870	0.7851	0.7830	0.7805	0.7794	0.7778	0.7772	0.7765	0.7757	0.7752	0.7817
22.1'	0.7855	0.8046	0.8021	0.8008	0.8021	0.7996	0.7976	0.7952	0.7926	0.7913	0.7896	0.7890	0.7881	0.7873	0.7868	0.7938
22.5'	0.7970	0.8174	0.8148	0.8134	0.8148	0.8121	0.8100	0.8075	0.8045	0.8032	0.8014	0.8008	0.7999	0.7988	0.7983	0.8057
22.9'	0.8083	0.8299	0.8272	0.8257	0.8271	0.8243	0.8220	0.8194	0.8163	0.8149	0.8130	0.8123	0.8114	0.8103	0.8097	0.8177
23.3'	0.8196	0.8422	0.8394	0.8378	0.8393	0.8364	0.8340	0.8313	0.8280	0.8266	0.8246	0.8238	0.8228	0.8217	0.8211	0.8295
23.7'	0.8307	0.8541	0.8512	0.8497	0.8512	0.8482	0.8457	0.8429	0.8395	0.8380	0.8359	0.8351	0.8341	0.8329	0.8322	0.8410
24.1'	0.8416	0.8656	0.8627	0.8611	0.8627	0.8596	0.8571	0.8542	0.8507	0.8492	0.8470	0.8462	0.8451	0.8439	0.8432	0.8523
24.5'	0.8523	0.8768	0.8739	0.8723	0.8738	0.8707	0.8682	0.8652	0.8616	0.8600	0.8578	0.8570	0.8559	0.8546	0.8539	0.8632
24.9'	0.8628	0.8876	0.8846	0.8830	0.8845	0.8814	0.8789	0.8759	0.8723	0.8707	0.8684	0.8676	0.8664	0.8652	0.8644	0.8739
25.3'	0.8730	0.8979	0.8950	0.8934	0.8949	0.8918	0.8893	0.8862	0.8826	0.8810	0.8788	0.8779	0.8767	0.8754	0.8747	0.8842
25.7'	0.8830	0.9078	0.9050	0.9034	0.9049	0.9018	0.8992	0.8962	0.8926	0.8910	0.8888	0.8879	0.8867	0.8854	0.8847	0.8942
26.1'	0.8928	0.9173	0.9145	0.9130	0.9144	0.9114	0.9089	0.9059	0.9023	0.9007	0.8985	0.8976	0.8965	0.8952	0.8944	0.9039
26.5'	0.9022	0.9264	0.9236	0.9222	0.9235	0.9206	0.9182	0.9152	0.9117	0.9101	0.9080	0.9071	0.9059	0.9046	0.9039	0.9133
26.9'	0.9115	0.9349	0.9323	0.9309	0.9322	0.9294	0.9271	0.9242	0.9207	0.9192	0.9171	0.9162	0.9151	0.9138	0.9131	0.9222
27.3'	0.9204	0.9430	0.9406	0.9392	0.9405	0.9378	0.9355	0.9328	0.9294	0.9279	0.9259	0.9250	0.9239	0.9227	0.9220	0.9309
27.7'	0.9290	0.9506	0.9484	0.9471	0.9482	0.9457	0.9435	0.9409	0.9377	0.9363	0.9343	0.9335	0.9324	0.9312	0.9305	0.9391
28.1'	0.9373	0.9578	0.9557	0.9545	0.9555	0.9532	0.9511	0.9486	0.9456	0.9442	0.9424	0.9416	0.9406	0.9394	0.9388	0.9469
28.5'	0.9453	0.9644	0.9625	0.9614	0.9624	0.9602	0.9583	0.9560	0.9531	0.9518	0.9501	0.9494	0.9484	0.9473	0.9467	0.9543
28.9'	0.9529	0.9705	0.9688	0.9678	0.9687	0.9667	0.9650	0.9628	0.9602	0.9590	0.9574	0.9567	0.9558	0.9548	0.9542	0.9613
29.3'	0.9602	0.9761	0.9746	0.9737	0.9744	0.9727	0.9711	0.9692	0.9668	0.9657	0.9643	0.9637	0.9628	0.9619	0.9613	0.9678
29.7'	0.9670	0.9811	0.9798	0.9791	0.9797	0.9782	0.9768	0.9751	0.9730	0.9720	0.9708	0.9702	0.9694	0.9686	0.9681	0.9739
30.1'	0.9735	0.9856	0.9845	0.9839	0.9844	0.9831	0.9820	0.9805	0.9786	0.9778	0.9767	0.9762	0.9756	0.9748	0.9744	0.9794
30.5'	0.9794	0.9895	0.9886	0.9882	0.9886	0.9875	0.9866	0.9853	0.9838	0.9831	0.9822	0.9818	0.9812	0.9806	0.9802	0.9844
30.9'	0.9849	0.9928	0.9922	0.9918	0.9921	0.9913	0.9906	0.9896	0.9884	0.9878	0.9871	0.9868	0.9863	0.9858	0.9855	0.9889
31.3'	0.9897	0.9956	0.9951	0.9949	0.9951	0.9945	0.9939	0.9932	0.9923	0.9919	0.9914	0.9911	0.9908	0.9904	0.9901	0.9927
31.7'	0.9939	0.9977	0.9974	0.9972	0.9974	0.9970	0.9967	0.9962	0.9956	0.9954	0.9950	0.9949	0.9946	0.9944	0.9942	0.9959
32.09	0.9973	0.9991	0.9990	0.9990	0.9990	0.9988	0.9987	0.9984	0.9982	0.9980	0.9979	0.9978	0.9977	0.9976	0.9975	0.9983
32.5'	0.9996	0.9999	0.9999	0.9999	0.9999	0.9999	0.9998	0.9998	0.9998	0.9998	0.9997	0.9997	0.9997	0.9997	0.9996	0.9998

as in Moon's computations [5]. While the figures listed apply strictly to only the March 7, 1970 total eclipse, they may be approximately scaled to other eclipses by multiplying the angular center-to-center distances in the table by the ratio (angular radius of moon in minutes of arc + angular radius of sun in minutes of arc)/32.55.

References

1. GRINGORTEN, I. I., and A. J. KANTOR: Handbook of Geophysics and Space Environments, ed. SHEA L. VALLEY, p. 3—17. New York: McGraw-Hill, 1965.
2. OUTCALT, S. I.: Water Resources Research, **5,** 1377 (1969).
3. ALLEN, C. W.: Astrophysical Quantities. 2nd edition, p. 170, London: Athlone Press, 1963.

4. DUNCOMBE, J. S.: U. S. Naval Observatory Circular, no. 125 (1969).
5. MOON, P.: Proposed Standard Solar Radiation Curves for Engineering Use. J. Frankling Institute, **230**, p. 583, 1940.

Authors' address: Dr. S. I. OUTCALT, Department of Geography, University of Michigan, Ann Arbor, MI 48104; Dr. D. D. MEISEL, Department of Physics, State University College, Geneseo, NY 14454, U. S. A.